available at www.sciencedirect.com

ScienceDirect

journal homepage: www.intl.elsevierhealth.com/journals/dema

Efficient 3D finite element analysis of dental restorative procedures using micro-CT data

Pascal Magne *

University of Southern California, Division of Primary Oral Health Care, School of Dentistry, 925 West 34th Street, DEN 4366, Los Angeles, CA 90089-0641, United States

ARTICLE INFO

Article history:
Received 3 November 2005
Received in revised form
23 March 2006
Accepted 27 March 2006

Keywords:
Finite element analysis
Restorative dentistry
Cuspal flexure
Composite resins
Porcelain inlays

ABSTRACT

Objectives. This investigation describes a rapid method for the generation of finite element models of dental structures and restorations.

Methods. An intact mandibular molar was digitized with a micro-CT scanner. Surface contours of enamel and dentin were fitted following tooth segmentation based on pixel density using an interactive medical image control system. Stereolithography (STL) files of enamel and dentin surfaces were then remeshed to reduce mesh density and imported in a rapid prototyping software, where Boolean operations were used to assure the interfacial mesh congruence (dentinoenamel junction) and simulate different cavity preparations (MO/MOD preparations, endodontic access) and restorations (feldspathic porcelain and composite resin inlays). The different tooth parts were then imported in a finite element software package to create 3D solid models. The potential use of the model was demonstrated using nonlinear contact analysis to simulate occlusal loading. Cuspal deformation was measured at different restorative steps and correlated with existing experimental data for model validation and optimization.

Results. Five different models were validated by existing experimental data. Cuspal widening (between mesial cusps) at 100 N load ranged from 0.4 μm for the unrestored tooth, 9–12 μm for MO, MOD cavities, to 12–21 μm for endodontic access cavities. Placement of an MOD adhesive restoration in porcelain resulted in 100% cuspal stiffness recovery (0.4 μm of cuspal widening at 100 N) while the composite resin inlay allowed for a partial recuperation of cusp stabilization (1.3 μm of cuspal widening at 100 N).

Significance. The described method can generate detailed and valid three dimensional finite element models of a molar tooth with different cavities and restorative materials. This method is rapid and can readily be used for other medical (and dental) applications.

1. Introduction

It is a well-established claim that mechanical testing is of paramount importance, not only in aerospace, civil engineering and the automotive industry, but also in health care. The field of biomedical research raises specific problems due to the fact that today's research may prove extremely expensive and ethically questionable when performed on live subjects. To limit the costs and risks involved in live experiments, virtual models and simulation approaches have become unavoidable [1]: an iterative optimization of the design of the experiment is performed on the computer and is seen in virtual prototyping and virtual testing and evaluation; after this iterative step, when the best design has been refined, the actual experiment

* Tel.: +213 740 4239; fax: +213 740 6778.
E-mail address: magne@usc.edu.

0109-5641/$ – see front matter © 2006 Academy of Dental Materials. Published by Elsevier Ltd. All rights reserved.
doi:10.1016/j.dental.2006.03.013

is conducted. The value is that the modeling and simulation step saves time and money for conducting the live experiment or clinical trial.

Yet dental research seems to make very little use of virtual models, such approaches representing a minor part of the scientific publication volume. In finite element (FE) analysis, a large structure is divided into a number of small simple-shaped elements, for which individual deformation (strain and stress) can be more easily calculated than for the whole undivided large structure. By solving the deformation of all the small elements simultaneously, the deformation of the structure as a whole can be assessed. Using the traditional biophysical knowledge database in a rational validation process [2], the use of FE analysis in dental research has been significantly refined during the last decade [3–10]. Nowadays, experimental–numerical approaches undoubtedly represent the most comprehensive in vitro investigation methods in restorative dentistry [9,10]. They allow the researcher (1) to reduce the time and cost required to bring a new idea from concept to clinical application, (2) to increase their confidence in the final concept/project by virtually testing it under all conceivable loading conditions.

Because teeth and bones cannot be assimilated to a simplified geometric representation but have anatomical shapes and a layered structure, sophisticated techniques have been developed to refine geometry acquisition, such as the recreation and digitization of planar outlines of the spatial anatomy [11,12]. This is often the most time-consuming step for the modeler. In addition, this process is prone to errors and simplifications which may induce faulty predictions. For this reason, patient's geometry-based meshing algorithms have already been proposed to generate complex solid models of bones as for example the CT scan-based FE model [6]. Similar approaches can be used with microscale CT scanner for the simulation of small objects like teeth, dental implants and dental restorations [13]. However, considerable work is still required in order to obtain congruent parts (sharing the exact same geometry at their interface) and smooth relationships between the different 3D objects (enamel, dentin, restoration). By the same token, modification of a given parameter, like for instance variations in restoration size, often requires the realization of a new and separate model, including the time-consuming geometry acquisition.

The aim of the present study is therefore to propose a further development to facilitate and accelerate geometry acquisition/modification during the fabrication of FE models of tooth restorations. The presented method is based on stereolithography (STL) and surface-driven automatic meshing. In this innovative approach, validated by cuspal flexure measurements, the model is built in multi-parts (using segmentation and Boolean operations with CAD objects) based on the geometry of the unaltered tooth. The same method can also be used to create patient-specific models from any other body part using either MRI or CT data.

Table 1 – Sequential procedure, computer software and times used to generate the 3D FE tooth model

1. Micro-CT scan data (stack of bitmap files) from Skyscan 1072 (Skyscan)

Scan time: 2 hours for 1128 slices

↓

2. Segmentation of enamel and dentin into 3-D objects (Mimics 9.0 + Remesh module, Materialise)

Generation of triangulated stereolithography files (STL) for enamel and dentin

Remeshing of STL files (triangle reduction, triangle quality improvement)

Accomplished in ca. 90 minutes

↓

3. STL files treatment (Magics 9.9, Materialise)

Boolean operations to ensure dentinoenamel mesh congruence

Boolean operations with CAD objects to simulate successive restorative procedures

Accomplished in ca. 30-60 minutes per model (including all Boolean operations)

↓

4. Automatic generation of volumetric mesh (MSC.Marc/Mentat 2005, MSC.Software)

Attribution of material properties and boundary conditions

Linear or nonlinear finite element analysis (e.g. contact analysis)

Accomplished in ca. 30-60 minutes per model (including 17 minutes to run the analysis)

The tooth model may be accomplished by a trained operator in less than a workday (depending of the complexity of the parts and general goal of the project). The same approach is applicable to other disciplines (orthodontics, orthopedic surgery, etc.) to generate patient-specific models from MRI or CT-scan data.

2. Materials and methods

2.1. *Mesh generation and material properties (pre-processing)*

A 4-step procedure (Table 1) was followed to generate a 3D FE model of an extracted human mandibular molar.

First, the tooth was scanned with Skyscan 1072 high resolution Micro-CT (Skyscan, Aartselaar, Belgium) with a voxel dimension of 13.65 μm. Exposure time was 7.2 s per frame, two frames were taken per angle and there were 208°. A total of 1128 slices were taken in 2 h. Only 81 slices (one slice out of every 14 slices) were used for the modeling.

Second, the different hard tissues visible on the scans were identified using an interactive medical image control system (MIMICS 9.0, Materialise, Leuven, Belgium). MIMICS imports CT and MRI data in a wide variety of formats and allows extended visualization and segmentation functions based on image density thresholding (Fig. 1A). 3D objects

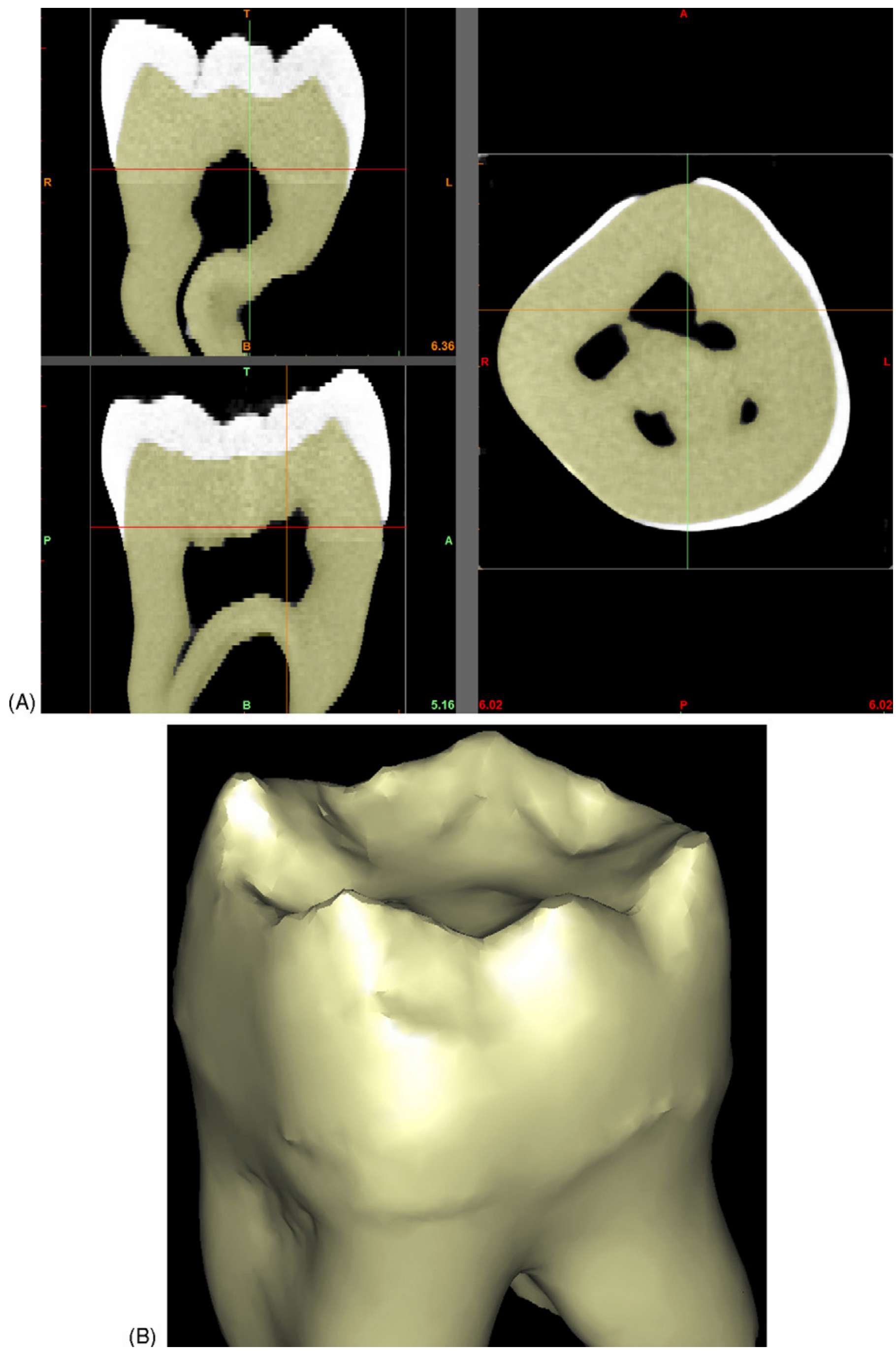

Fig. 1 – (A) CT-scan data as seen in MIMICS 9.0. The tooth is presented in three different cross-sectional views. Masks have been applied to enamel (white) and dentin (yellow) according to voxel density thresholding. (B) 3D representation of dentin as a result of segmentation in MIMICS.

(enamel and dentin) are automatically created in the form of masks by growing a threshold region on the entire stack of scans (Fig. 1B). Using MIMICS STL+ module, enamel (Fig. 2A) and dentin were then separately converted into stereolithography files (STL, bilinear and interplane interpolation algorithm). Native STLs are improper for use in FEA because of the aspect ratio and connectivity of the triangles in these files. The REMESH module attached to MIMICS was therefore used to automatically reduce the amount of triangles and simultaneously improve the quality of the triangles while maintaining the geometry (Fig. 2B). During remesh, the tolerance variation from the original data can be specified (quality of triangles does not mean tolerance variation from the original data). The quality is defined as a measure of triangle height/base ratio so that the file can be imported in the finite element anal-

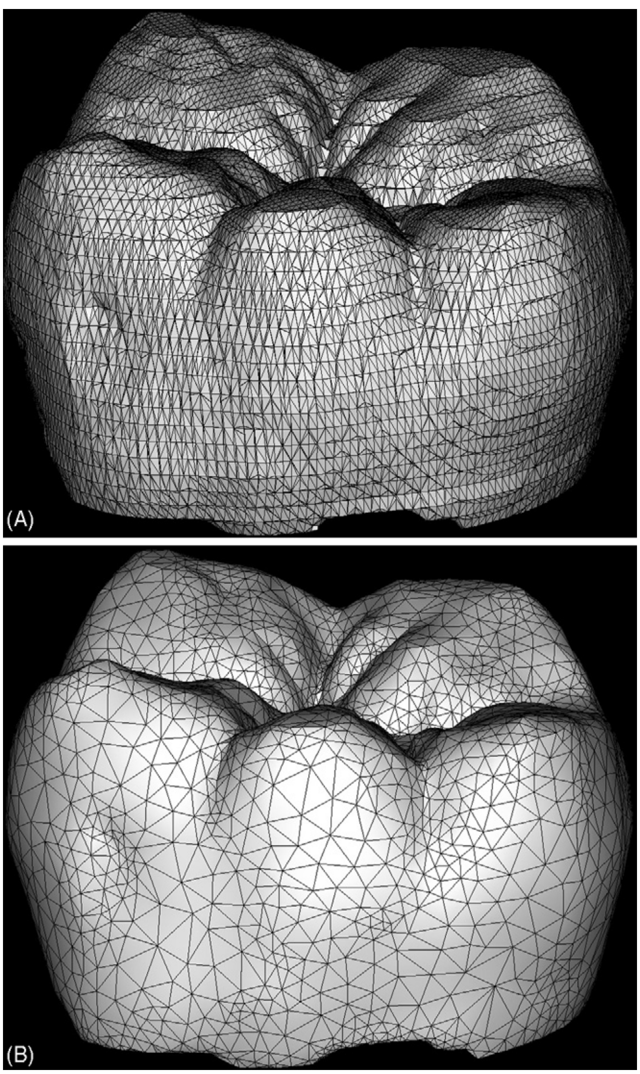

Fig. 2 – (A) Stereolithography triangulated (STL) file of enamel obtained through the STL+ module within MIMICS. The density and quality (aspect ratio and connectivity) of the triangles is not appropriate for use in finite element analysis. (B) Enamel STL file optimized for FEA using the REMESH module within MIMICS. Note the improved triangle shape and the intact geometry compared to Fig. 2A in spite of a significant reduction in number of triangles.

Table 2 – FEA geometry and characteristics for the different models

Model label	Description	Specific features	Volumetric mesh	
			No. of elements[a]	No. of nodes[a]
NAT	Intact natural tooth (unrestored)	Mandibular molar	129374	27223
CAV_MO	Unrestored tooth with MO preparation	Occlusal width: 1/2 intercusp. width; occlusal depth: >3 mm; proximal depth: 1 mm above CEJ; distal marginal ridge intact	106817	23519
CAV_MOD	Unrestored tooth with MOD preparation	Occlusal width: 1/2 intercusp. width; occlusal depth: >3 mm; proximal depth: 1 mm above CEJ	95826	21510
ENDO_MO	Unrestored tooth with MO preparation and endodontic access preparation	Endodontic access cavity removing intact wall with adjacent box.	113603	25554
ENDO_MOD	Unrestored tooth with MOD preparation and endodontic access preparation	Endodontic access cavity removing intact walls with both adjacent boxes	102612	23432
CPR	Tooth restored with MOD composite restoration	Restoration size similar to CAV	129374	27223
CER	Tooth restored with MOD feldspathic ceramic restoration	Restoration size similar to CAV	129374	27223

[a] Stone base excluded.

ysis software package without generating any problem. The remesh operations were also applied to the dentin STL. Segmentation of enamel and dentin may be accomplished by a trained operator in ca. 90 min (including remesh of the STL files).

Third, a strereolithography handling software (MAGICS 9.9, Materialise, Leuven Belgium) was used in order to reestablish the congruence of the interfacial mesh between enamel and dentin (this congruence being lost during the previous remeshing process) using Boolean operations (addition, intersection or subtraction of volumes). Once a congruent mesh at the dentinoenamel junction was obtained (Fig. 3A), additional Boolean operations with CAD objects (Fig. 3B and C) were used to simulate a cylindrical fixation base (embedding the root within 2 mm of the cementoenamel junction), as well as different cavity preparations (MO and MOD cavities, endodontic access cavities) and restorations. The exact design and dimensions of the MO, MOD and endodontic access cavities are described in Table 2. These successive restorative situations were chosen because they reproduce existing experiments

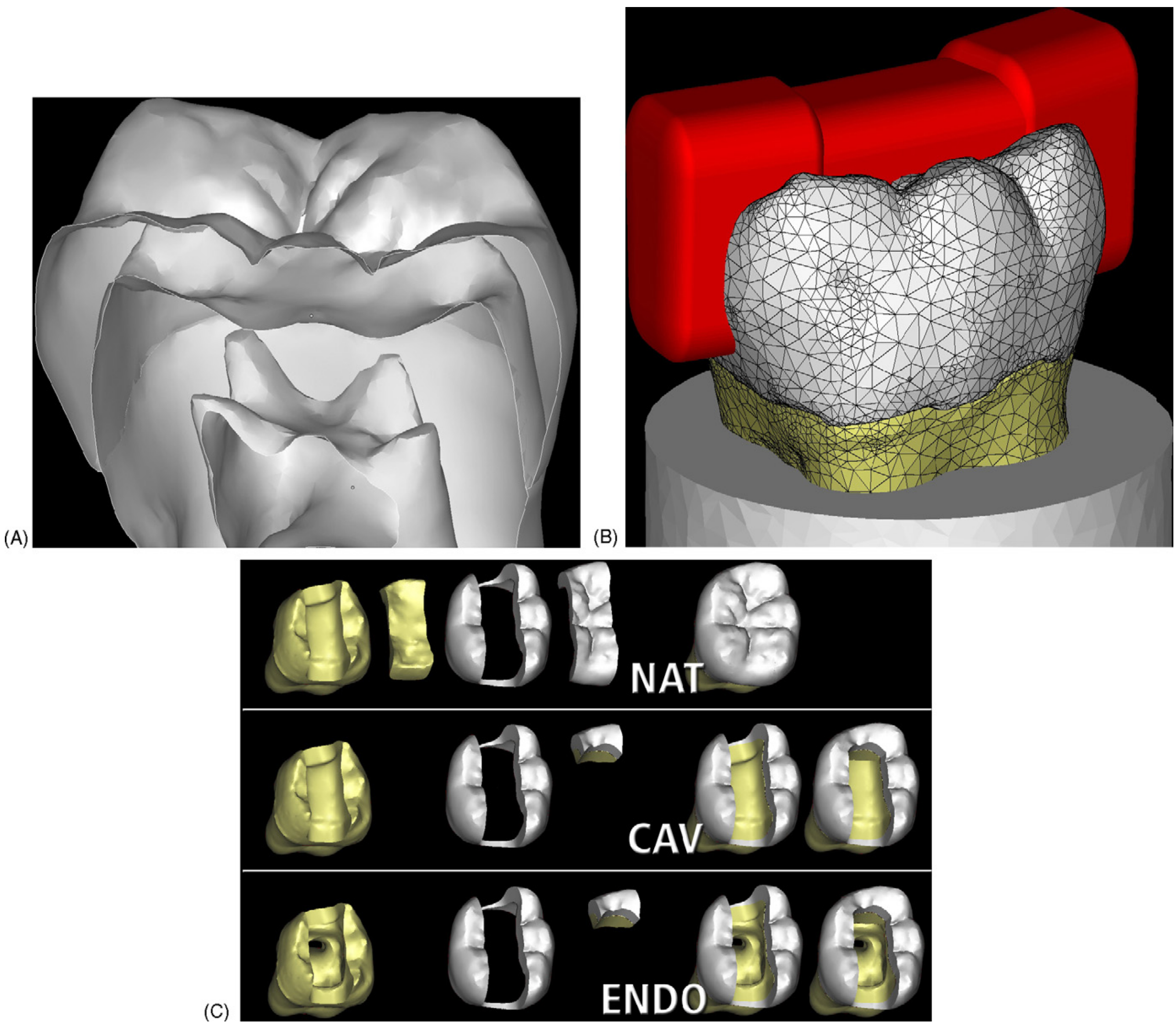

Fig. 3 – (A) Cross-sectional view of the enamel–dentin assembly as seen in MAGICS. Both enamel and dentin STLs share the exact same geometry at their interface (dentinoenamel junction). (B). Congruent enamel (white) and dentin (yellow) meshes along with CAD objects used to simulate a stone base (cylinder) and different cavity designs (red inserts). Mesh congruence between the root portion and the stone base was obtained through a Boolean subtraction process (stone cylinder minus dentin). (C). Congruent STL parts of enamel (white) and dentin (yellow) resulting from Boolean intersections and substractions between the original enamel/dentin STLs and different CAD inserts (right side). The assembly of the different parts result in five possible models (left side), i.e. the natural tooth (NAT), MO and MOD cavities (CAV), MO and MOD endodontic access preparations (ENDO). The NAT model was also used to simulate a composite resin inlay (CPR) and a porcelain inlay (CER) by attributing different material properties to the enamel and dentin inserts (see Table 2).

Table 3 – Material properties

	Elastic modulus (GPa)	Poisson's ratio
Enamel	84.1[a]	0.30[b]
Dentin	18.6[c]	0.31[d]
Composite	10.0[e]	0.24[f]
Ceramic	78.0[g]	0.28[a]

[a] Craig et al. [25].
[b] Anusavice and Hojjatie [24].
[c] McGuiness et al. [28].
[d] Farah et al. [27].
[e] Eldiwany et al. [26].
[f] Nakayama et al. [29].
[g] Data from manufacturer of Creation-Willi Geller dental porcelain (Klema, Meiningen, Austria).

[14–16], which will be used in the validation process of the FEA model (see Section 3). Two additional experimental conditions were generated by attributing different material properties to the enamel and dentin inserts included in model NAT: a composite resin inlay (CPR) and a feldspathic ceramic inlay (CER). The treatment of the STL files in MAGICS may be accomplished by a trained operator in ca. 30–60 min per model (including all Boolean operations).

Fourth, the optimized STL files of the segmented enamel and dentin parts were then imported in a finite element analysis software package (MSC.Marc/MSC.Mentat, MSC.Software, Santa Ana, CA) for the generation of a volumetric mesh and attribution of material properties (Table 3). The triangulated STL files are ideal for automatic mesh generation using a tetrahedral mesher (tetrahedron elements with pyramid-like shape and 4 nodal points). This last step may be accomplished by a trained operator in ca. 30–60 min per model (including attribution of boundary conditions and 17 min to run the analysis).

2.2. *Boundary conditions, loadcase and data processing*

Fixed zero-displacement in the three spatial dimensions was assigned to the nodes at the bottom surface of the stone base. The tooth and restorative materials were taken as bonded, which simulate usage of adhesive luting cements. A uniformly ramp loading was applied to the mesial cusps through a rigid body, i.e. a 9.5-mm diameter ball positioned as close as possible to the tooth (Fig. 4). The tooth was defined as deformable contact body. Contact between these bodies was determined automatically by the FEA simulation during the static mechanical loadcase (no inertia effects) with a uniform stepping procedure of 10 steps. A motion was applied to the rigid ball along the Z-axis through a negative velocity of 0.02 mm per step. Only one step was required to reach contact in both cusps. The motion continued for the remaining steps to reach a total force 100–200 N on the ball (depending on the model). The stress and strain distributions were solved using the MSC.Marc solver. As mentioned before, these specific boundary conditions, load protocol and configuration were chosen because they reproduce existing experiments by Panitvisai and Messer [14], and Jantarat et al. [15,16].

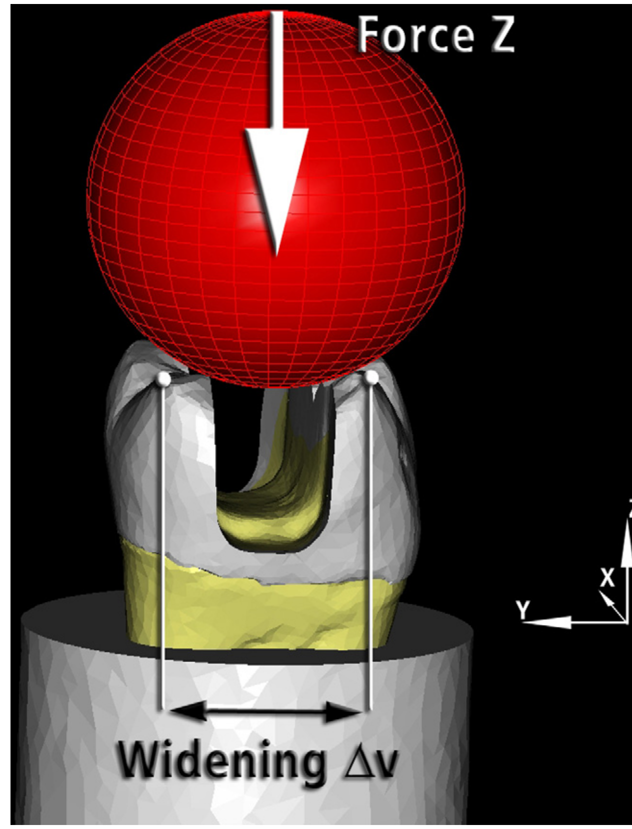

Fig. 4 – Load protocol and configuration as seen in Mentat, i.e. a nonlinear contact analysis between a rigid body (9.5-mm diameter load sphere moving along Z-axis against the tooth) and a deformable tooth (CAV_MOD shown here). The widening of the cusps (Δv) was calculated from the output values of displacement along the Y-axis for selected nodes near the cusp tip.

3. Results

The post-processing file was accessed through MENTAT to select specific nodes on the buccal and lingual enamel near the cusp tip and to collect the values of displacement in the Y direction for each loading step ($Y+$ denotes displacement in lingual direction and $Y-$ in buccal direction). The force along the Z-axis on the rigid ball was also collected for each step. After the transfer of these data to a spreadsheet, the widening (deformation) of the cusp was calculated (by summing the displacement of each cusp) and plotted against the force along Z-axis on the ball (Fig. 5). As expected in an elastic simulation, there is a quasi-linear relationship between load and deformation. The progressive loss of tooth substance (MO to MOD to ENDO) translates into a progressive loss of cuspal stiffness (decreased slope of the force vs. deformation plot). The unrestored tooth (NAT) and the tooth with the MOD ceramic inlay (CER) display the same conduct (100% recovery of cuspal stiffness), while the more flexible composite inlay allowed for partial of recovery of cuspal stiffness.

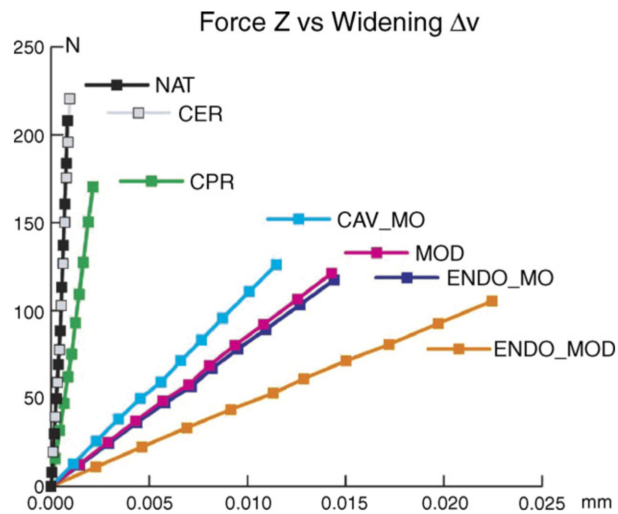

Fig. 5 – Force generated by the load ball in Newtons vs. cuspal widening in millimeters (mesial cusps) for each experimental design.

FEA validation

For validation of the models, the widening of the mesial cusp at a load of 100 N for all groups was extracted and is presented in Table 4 along with results from existing experiments by Panitvisai and Messer [14] and Jantarat et al. [15,16] who used the same type of tooth, loading protocol (static load at 100 N) and configuration (9.5 mm load sphere seating on the mesial cusps).

There is a good association between FEA and experimental values at each restorative step, the difference being inferior to 3 μm in most conditions. A larger difference was noted when comparing the MOD endodontic accesses in the FEA to the study by Panitvisai and Messer: [14] 21.3 μm versus 28.8 μm respectively. This discrepancy, however, does not appear when comparing the same model with the studies by Jantarat et al. [15,16] The MOD composite yielded 1.3 μm of cuspal widening (3× the value of NAT), unlike the MOD ceramic restoration, which was similar to the unaltered tooth (0.4 μm).

4. Discussion

A number of studies [17–20] analyzing biophysical stress and strain have shown that restorative procedures can make the tooth crown more deformable, and teeth could be strengthened by increasing their resistance to crown deformation. The standard loadcase applied in the present analysis constitutes the most discriminating technique to study crown deformation; it also constitutes a useful validation set-up that mirrors existing experimental cuspal flexure measurements. Jantarat et al. [16] used an extensometer and only measured teeth with an opened MOD endodontic access. Panitvisai and Messer [14] and Janatarat et al. [15] used direct current displacement transducers (DCDT) to measure individual cusp displacement. The precision of each transducer being around 1 μm, they were not able to measure submicron displacements. In addition, a cumulated error of 2 μm can be expected on the total cusp widening. The maximum difference found between the experimental measurements and the FEA model was around 3 μm. Considering that the inter-tooth variability reported by both articles far exceeds these values, the model can be considered valid. The results obtained with composite restored teeth (CPR) are in agreement with conclusions by Douglas [17] stating that their strength falls off with increasing cavity size and can only approach that of the unaltered tooth in the case of small conservative cavities. This cannot be said about ceramic restored teeth (CER), the behavior of which is strictly mimicking the unaltered tooth (Fig. 6). These results are in agreement with in vivo and in vitro studies [21,22] showing tooth-like fracture resistance, better cuspal protection and significantly better "anatomical form of the surface" and "integrity of the restoration" for ceramic inlays compared to composite ones.

As illustrated in the present article, the proposed approach resulted in valid 3D models with very detailed tooth anatomy and realistic computation process. Previous attempt to generate 3D models resulted in much coarser meshes [11,12], mainly due to the limitation of the geometry acquisition method (manual tracing of actual tooth sections), another reason being the increased memory requirements for 3D models, which did not allow fine representation of the geometry. Other authors [3–5] digitized a plaster model (crown portion) and extrapolated the inner geometry (pulp, root dentin and enamel volumes) using tooth morphology literature data. Different

Table 4 – Results and comparison with existing experimental data

Experimental condition	Widening Δv (μm) at 100 N load (force Z)			
	FEA	Panitvisai and Messer [14]	Jantarat et al.	
			[15]	[16]
NAT (intact tooth)	0.4	<1	<2	–
CAV_MO (MO cavity)	9.1	6	–	–
CAV_MOD (MOD cavity)	11.8	10	6–10	–
ENDO_MO (MO + endo. access)	12.3	14.4	–	–
ENDO_MOD (MOD + endo. access)	21.3	28.8	24–32	17–18
CER (MOD ceramic inlay)	0.4	–	–	–
CPR (MOD composite inlay)	1.3	–	–	–

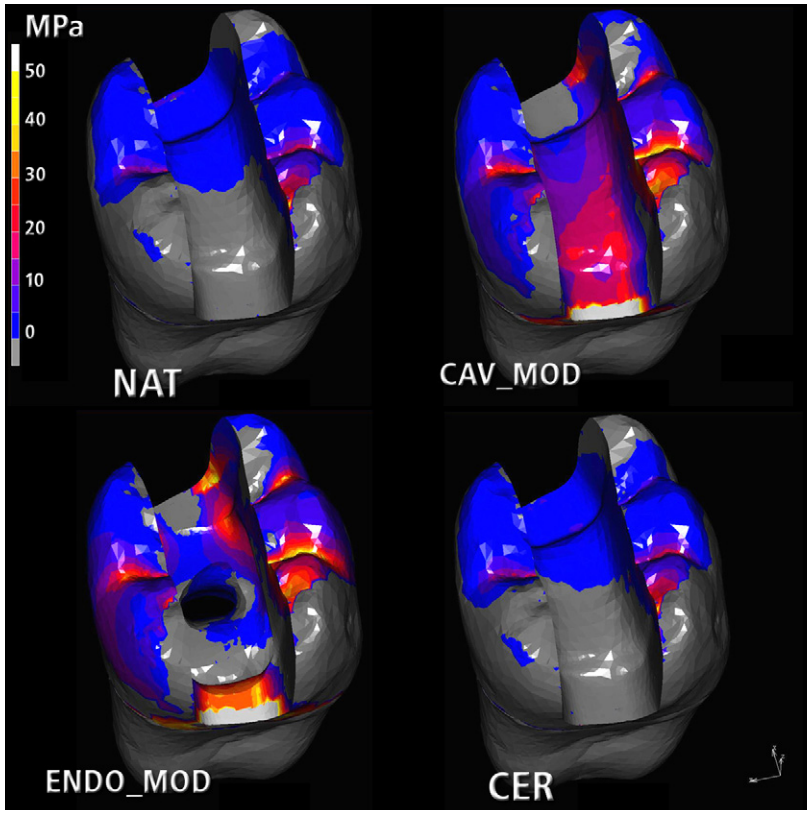

Fig. 6 – First principal stress distribution in four of the seven models studied. To allow for better comparison of the stress pattern, the MOD insert of enamel and dentin (model NAT) or the MOD ceramic restoration (model CER) were made invisible. Colors, tensile stresses; gray, compressive stresses. Note the similarity between NAT and CER.

approaches were proposed to access the inner anatomical detail without extrapolation and accelerate the production of the models. Verdonschot et al. [13] might have been the first authors to describe the development of a 3D finite element model of a restored tooth based on a microscale CT data-acquisition technique. The tooth was scanned after being restored with an MOD composite and the 3D geometry was obtained through the stacking of traced 2D sections, still involving a significant amount of manual work. An interesting semi-automated method was proposed [6–8] to generate solid models of bones without internal boundaries (plain automatic volumetric mesh), then using the Hounsfield unit (HU) to attribute a specific Young's modulus to each element based on scan density. When applied to small structures like teeth (with thin anatomical details such as the enamel shell), this technique does not allow the fine control of internal boundaries (e.g. dentinoenamel junction), the exact geometry of which will have to follow the automatic volumetric meshing process.

The approach used in the present study suggests that maximum anatomical detail is obtained by surface/interface-based meshing using stereolithography (STL) surface data. The different parts of the model featuring different mechanical properties are identified first (segmentation process) and meshed accordingly. Elements do not overlap the different structures but strictly follow the internal boundaries, resulting in a smooth and very well controlled representation of interfaces like the dentinoenamel junction (Fig. 3A). Significant advantages, when using STLs, are the sophisticated visualization tools (shaded wireframe 3D views, section views etc.) and possibilities offered by the Boolean operations. The general principle of Boolean operations is that a new object can be formed by combining two 3D objects. Objects can be united, intersected or subtracted. When intersecting or subtracting two overlapping objects, a congruent mesh is assured at the interface between the new objects. This property is essential to assure the continuity of the resulting volumetric mesh. Boolean operations with predefined CAD objects (box, cylinder, cone or inserts as in Fig. 3B) constitute an important feature. It allowed us to "digitally" simulate successive restorative procedures (Fig. 3C), unlike Verdonschot et al. [13] who had to "physically" restore the tooth before scanning it. In the present study, the geometry of the unaltered tooth remains, allowing for direct comparison with the different experimental conditions. The very user-friendly graphic interface allows for rapid modifications of the different parts and generations of new STLs that can be instantly exported and volumetrically meshed the FEA program. It must be pointed out that micro-CT is not suitable for human teeth in live patients. However, considering that only 81 slices were necessary to generate these valid FEA models, one can easily foresee that the exponential development of commercial dental CT-scanners, computer processing power and interface friendliness will make this approach even faster and more automated, allowing the rapid fabrication of patient-specific simulation of dental restorations in a very near future. Even though small differences may remain between the reality and the finite element environment, numerical modeling is able to reveal the otherwise inaccessible stress distribution within the tooth-restoration complex (Fig. 6) and it has proven to be a useful tool in the thinking process for the understanding of tooth biomechanics and the biomimetic approach in restorative dentistry [23].

5. Conclusion

This investigation describes a rapid method for the generation of finite element models of dental structures and restorations. Detailed three dimensional finite element models of a molar tooth with different cavities and restorative materials were generated. The potential use of the model was demonstrated using nonlinear contact analysis to simulate occlusal loading. Cuspal widening was measured at different restorative steps and correlated with existing experimental data for model validation and optimization. This method is rapid (a tooth model may be obtained by a skilled operator in less than a workday) and can readily be used for other medical applications to create patient-specific models from any other body part using either MRI or CT data. Further, this methodology could facilitate optimization and understanding of biomedical devices prior to animal and human clinical trials.

Acknowledgements

The author wish to express his gratitude to Tim Sledz (Micro Photonics Inc., distributor of Skyscan in the USA) for scanning the experimental sample. This study was supported in part by MSC.Software (MSC.Marc/MSC.Mentat products) and Materialise (MIMICS/MAGICS products). Special thanks to Dan Wolf (MSC.Software) for helpful suggestions and Mrs. Constance Nelson who has given in memory of Dr. Gus Swab.

REFERENCES

[1] Satava RM. The scientific method is dead—long live the (new) scientific method. Surg Innov 2005;12:173–6.
[2] Korioth TW, Versluis A. Modeling the mechanical behavior of the jaws and their related structures by finite element (FE) analysis. Crit Rev Oral Biol Med 1997;8:90–104.
[3] Ausiello P, Apicella A, Davidson CL, Rengo S. 3D-finite element analyses of cusp movements in a human upper premolar, restored with adhesive resin-based composites. J Biomech 2001;34:1269–77.
[4] Ausiello P, Apicella A, Davidson CL. Effect of adhesive layer properties on stress distribution in composite restorations—a 3D finite element analysis. Dent Mater 2002;18:295–303.
[5] Ausiello P, Rengo S, Davidson CL, Watts DC. Stress distributions in adhesively cemented ceramic and resin-composite class II inlay restorations: a 3D-FEA study. Dent Mater 2004;20:862–72.
[6] Cattaneo PM, Dalstra M, Frich LH. A three-dimensional finite element model from computed tomography data: a semi-automated method. Proc Inst Mech Eng [H] 2001;215:203–13.
[7] Cattaneo PM, Dalstra M, Melsen B. The transfer of occlusal forces through the maxillary molars: a finite element study. Am J Orthod Dentofacial Orthop 2003;123:367–73.
[8] Cattaneo PM, Dalstra M, Melsen B. The finite element method: a tool to study orthodontic tooth movement. J Dent Res 2005;84:428–33.
[9] Tantbirojn D, Versluis A, Pintado MR, DeLong R, Douglas WH. Tooth deformation patterns in molars after composite restoration. Dent Mater 2004;20:535–42.
[10] Versluis A, Tantbirojn D, Pintado MR, DeLong R, Douglas WH. Residual shrinkage stress distributions in molars after composite restoration. Dent Mater 2004;20:554–64.
[11] Lin CL, Chang CH, Wang CH, Ko CC, Lee HE. Numerical investigation of the factors affecting interfacial stresses in an MOD restored tooth by auto-meshed finite element method. J Oral Rehabil 2001;28:517–25.
[12] Lin CL, Chang CH, Ko CC. Multifactorial analysis of an MOD restored human premolar using auto-mesh finite element approach. J Oral Rehabil 2001;28:576–85.
[13] Verdonschot N, Fennis WM, Kuijs RH, Stolk J, Kreulen CM, Creugers NH. Generation of 3D finite element models of restored human teeth using micro-CT techniques. Int J Prosthodont 2001;14:310–5.
[14] Panitvisai P, Messer HH. Cuspal deflection in molars in relation to endodontic and restorative procedures. J Endod 1995;21:57–61.
[15] Jantarat J, Panitvisai P, Palamara JE, Messer HH. Comparison of methods for measuring cuspal deformation in teeth. J Dent 2001;29:75–82.
[16] Jantarat J, Palamara JE, Messer HH. An investigation of cuspal deformation and delayed recovery after occlusal loading. J Dent 2001;29:363–70.
[17] Douglas WH. Methods to improve fracture resistance of teeth. In: Vanherle G, Smith DC, editors. International symposium on posterior composite resin restorative materials. Symposium sponsored by 3M, St. Paul, MN. The Netherlands: Peter Szulc Publishing Company; 1995. p. 433–41.
[18] Hood JAA. Methods to improve fracture resistance of teeth. In: Vanherle G, Smith DC, editors. International symposium on posterior composite resin restorative materials. Symposium sponsored by 3M, St. Paul, MN. The Netherlands: Peter Szulc Publishing Company; 1995. p. 443–50.
[19] Morin DL, Douglas WH, Cross M, DeLong R. Biophysical stress analysis of restored teeth: experimental strain measurements. Dent Mater 1988;4:41–8.
[20] Morin DL, Cross M, Voller VR, Douglas WH, DeLong R. Biophysical stress analysis of restored teeth: modeling and analysis. Dent Mater 1988;4:77–84.
[21] Manhart J, Chen HY, Neuerer P, Scheibenbogen-Fuchsbrunner A, Hickel R. Three-year clinical evaluation of composite and ceramic inlays. Am J Dent 2001;14:95–9.
[22] Mehl A, Kunzelmann KH, Folwaczny M, Hickel R. Stabilization effects of CAD/CAM ceramic restorations in extended MOD cavities. J Adhes Dent 2004;6:239–45.
[23] Magne P, Belser U. Bonded porcelain restorations in the anterior dentition—a biomimetic approach. Chicago: Quintessence Publishing Co.; 2002.
[24] Anusavice KJ, Hojjatie B. Influence of incisal length of ceramic and loading orientation on stress distribution in ceramic crowns. J Dent Res 1988;67:1371–5.
[25] Craig RG, Peyton FA, Johnson DW. Compressive properties of enamel, dental cements, and gold. J Dent Res 1961;40:936–45.
[26] Eldiwany M, Powers JM, George LA. Mechanical properties of direct and post-cured composites. Am J Dent 1993;6:222–4.

[27] Farah JW, Craig RG, Meroueh KA. Finite element analysis of three- and four-unit bridges. J Oral Rehabil 1989;16:603–11.
[28] McGuiness NJ, Wilson AN, Jones ML, Middleton J. A stress analysis of the periodontal ligament under various orthodontic loadings. Eur J Orthod 1991;13:231–42.
[29] Nakayama WT, Hall DR, Grenoble DE, Katz JL. Elastic properties of dental resin restorative materials. J Dent Res 1974;53:1121–6.